

MIT Open Access Articles

Preparation and transmission of low-loss azimuthally polarized pure single mode in multimode photonic band gap fibers

The MIT Faculty has made this article openly available. **Please share** how this access benefits you. Your story matters.

Citation: Shemuly, Dana, Alexander M. Stolyarov, Zachary M. Ruff, Lei Wei, Yoel Fink, and Ofer Shapira. "Preparation and transmission of low-loss azimuthally polarized pure single mode in multimode photonic band gap fibers." *Optics Express* 20, no. 6 (February 27, 2012): 6029. © 2012 Optical Society of America

As Published: <http://dx.doi.org/10.1364/OE.20.006029>

Publisher: Optical Society of America

Persistent URL: <http://hdl.handle.net/1721.1/79621>

Version: Final published version: final published article, as it appeared in a journal, conference proceedings, or other formally published context

Terms of Use: Article is made available in accordance with the publisher's policy and may be subject to US copyright law. Please refer to the publisher's site for terms of use.



Preparation and transmission of low-loss azimuthally polarized pure single mode in multimode photonic band gap fibers

Dana Shemuly,¹ Alexander M. Stolyarov,¹ Zachary M. Ruff,² Lei Wei,¹ Yoel Fink,¹ and Ofer Shapira^{1,*}

¹Research Laboratory of Electronics, Massachusetts Institute of Technology, 77 Massachusetts Avenue, Cambridge, Massachusetts 02329-0407, USA

²OmniGuide, One Kendall Sq. building 100, 3rd floor, Cambridge, Massachusetts 02139, USA

*ofers@mit.edu

Abstract: We demonstrate the preparation and transmission of the lowest loss azimuthally polarized TE₀₁-like mode in a photonic band gap (PBG) fiber. Using the nature of the mode and the properties of the band gap structure we construct a novel coupler that operates away from the band gap's center to enhance the differential losses and facilitate the radiative loss of hybrid fundamental fiber modes. Remarkably, even though the coupler is highly multimoded, a pure azimuthally polarized mode is generated after only 17cm. Theoretical calculations verify the validity of this technique and accurately predict the coupling efficiency. The generation and single mode propagation of this unique azimuthally polarized, doughnut shaped mode in a large hollow-core fiber can find numerous applications including in optical microscopy, optical tweezers, and guiding particles along the fiber.

© 2012 Optical Society of America

OCIS codes: (060.2310) Fiber optics; (060.5295) Photonic crystal fibers; (230.7370) Waveguides.

References and links

1. W. L. Barrow, "Transmission of electromagnetic waves in hollow metal tubes," *Proc. IRE* **24**, 1298–1328 (1936).
2. J. R. Carson, S. P. Mead, and S. A. Schelkunoff, "Hyper-frequency wave guides—mathematical theory," *Bell Syst. Tech. J.* **15**, 310–333 (1936).
3. O. Shapira, A. F. Abouraddy, Q. Hu, D. Shemuly, J. D. Joannopoulos, and Y. Fink, "Enabling coherent superpositions of iso-frequency optical states in multimode fibers," *Opt. Express* **18**(12), 12622–12629 (2010).
4. T. G. Euser, G. Whyte, M. Scharrer, J. S. Y. Chen, A. Abdolvand, J. Nold, C. F. Kaminski, and P. St. J. Russell, "Dynamic control of higher-order modes in hollow-core photonic crystal fibers," *Opt. Express* **16**(22), 17972–17981 (2008).
5. F. K. Fatemi, M. Bashkansky, E. Oh, and D. Park, "Efficient excitation of the TE₀₁ hollow metal waveguide mode for atom guiding," *Opt. Express* **18**(1), 323–332 (2010).
6. Y. Yirmiyahu, A. Niv, G. Biener, V. Kleiner, and E. Hasman, "Excitation of a single hollow waveguide mode using inhomogeneous anisotropic subwavelength structures," *Opt. Express* **15**(20), 13404–13414 (2007).
7. M. Skorobogatiy, C. Anastassiou, S. G. Johnson, O. Weisberg, T. Engeness, S. Jacobs, R. Ahmad, and Y. Fink, "Quantitative characterization of higher-order mode converters in weakly multimoded fibers," *Opt. Express* **11**(22), 2838–2847 (2003).
8. O. Shapira, A. F. Abouraddy, J. D. Joannopoulos, and Y. Fink, "Complete modal decomposition for optical waveguides," *Phys. Rev. Lett.* **94**(14), 143902 (2005).
9. B. Temelkuran, S. D. Hart, G. Benoit, J. D. Joannopoulos, and Y. Fink, "Wavelength-scalable hollow optical fibres with large photonic bandgaps for CO₂ laser transmission," *Nature* **420**(6916), 650–653 (2002).
10. D. Shemuly, Z. M. Ruff, A. M. Stolyarov, G. Spektor, S. G. Johnson, Y. Fink, and O. Shapira are preparing a manuscript to be called "Asymmetric wave propagation in planar chiral fibers."
11. P. Yeh, A. Yariv, and E. Marom, "Theory of Bragg fiber," *J. Opt. Soc. Am.* **68**(9), 1196–1201 (1978).
12. S. G. Johnson, M. Ibanescu, M. Skorobogatiy, O. Weisberg, T. Engeness, M. Soljacic, S. Jacobs, J. D. Joannopoulos, and Y. Fink, "Low-loss asymptotically single-mode propagation in large-core OmniGuide fibers," *Opt. Express* **9**(13), 748–779 (2001).

13. M. J. Renn, D. Montgomery, O. Vdovin, D. Z. Anderson, C. E. Wieman, and E. A. Cornell, "Laser-guided atoms in hollow-core optical fibers," *Phys. Rev. Lett.* **75**(18), 3253–3256 (1995).
14. Z. Wang, M. Dai, and J. Yin, "Atomic (or molecular) guiding using a blue-detuned doughnut mode in a hollow metallic waveguide," *Opt. Express* **13**(21), 8406–8423 (2005).
15. K. S. Youngworth and T. Brown, "Focusing of high numerical aperture cylindrical-vector beams," *Opt. Express* **7**(2), 77–87 (2000).
16. Q. Zhan and J. Leger, "Focus shaping using cylindrical vector beams," *Opt. Express* **10**(7), 324–331 (2002).
17. S. G. Johnson, P. Bienstman, M. A. Skorobogatiy, M. Ibanescu, E. Lidorikis, and J. D. Joannopoulos, "Adiabatic theorem and continuous coupled-mode theory for efficient taper transitions in photonic crystals," *Phys. Rev. E Stat. Nonlin. Soft Matter Phys.* **66**(6), 066608 (2002).
18. T. Grosjean, D. Courjon, and M. Spajer, "An all-fiber device for generating radially and other polarized light beams," *Opt. Commun.* **203**(1-2), 1–5 (2002).
19. M. Imai and E. H. Hara, "Excitation of the fundamental and low-order modes of optical fiber waveguides with gaussian beams. 2: offset beams," *Appl. Opt.* **14**(1), 169–173 (1975).
20. Z. Ruff, D. Shemuly, X. Peng, O. Shapira, Z. Wang, and Y. Fink, "Polymer-composite fibers for transmitting high peak power pulses at 1.55 microns," *Opt. Express* **18**(15), 15697–15703 (2010).
21. T. Engeness, M. Ibanescu, S. G. Johnson, O. Weisberg, M. Skorobogatiy, S. Jacobs, and Y. Fink, "Dispersion tailoring and compensation by modal interactions in OmniGuide fibers," *Opt. Express* **11**(10), 1175–1196 (2003).

The TE₀₁ mode of a cylindrical waveguide has a venerable history. Since its discovery in 1936 [1, 2] this mode has garnered attention because of its unique polarization state and the lower propagation losses. In fact, this mode has been shown to be the lowest loss mode in metallic waveguides. Unlike the doubly degenerate fundamental HE₁₁ mode, the lowest-loss TE₀₁ mode in PBG fibers is non-degenerate, alleviating polarization mode dispersion (PMD). Operating with this mode can offer a true single mode transmission and eliminate in principle the uncertainty associated with polarization rotation in transmission systems that are doubly degenerate.

Exciting a specific mode in a waveguide that supports a multiplicity of modes requires the generation of the mode's vectorial field profile. In previous studies, controlled coupling was achieved by altering the input beam to partially fit an eigenfunction of the waveguide using, for example, spatial light modulators [3–5], sub-wavelength polarization masks [6], or controlled deformation of the fiber [7, 8]. None of these techniques, though, has managed to fully match the eigenfunction in phase, polarization, and intensity. This imperfect match can lead to "parasitic" coupling of the light to unwanted modes that can be solved, in most cases, by a natural filtering effect of the waveguide or by limiting the number of modes in the waveguide.

Here we demonstrate a different approach to exciting distinct low-loss waveguide modes using PBG fibers. Instead of using external optical means to realize the fiber eigenfunction, we suggest using the fiber itself to generate a specific eigenfunction. Using the same fiber allows us to reconstruct the eigenfunction accurately in intensity, polarization, and phase. Moreover, by using a photonic band gap fiber as our waveguide, we utilize the properties of the modes in and out of the band gap to filter out unwanted modes, achieving only the desired mode at the output. After generating a beam with the exact modal characteristics at the output of the first fiber ("coupler"), we demonstrate the accurate coupling to a highly multi-mode fiber (a "test" fiber). Compared to previously proposed methods, our technique uses less costly optics and generates a more precise match to the desired optical mode.

Hollow-core one dimensional photonic band gap fibers (Bragg fibers) are made of alternating layers of high and low index-of-refraction materials. In our studies, the fibers are made by thermally drawing an air-core preform that is formed by rolling a chalcogenide glass coated polymer sheet [9]. This generates a spiral cross section that is made out of bilayers of low-index (polymer) and high-index (glass) materials. This spiral cross-section has many unique light propagation properties that were studied elsewhere [10]. However, for the purpose of this paper most of the differences between this fiber and the classic Bragg fiber are of less importance, since the spiral fiber shares many fundamental properties with the concentric Bragg fiber: the existence of a band gap, the properties of the modes in and out of

the band gap, and the general characteristics of the modes [11, 12]. Throughout the paper, we will highlight the differences that arise due to the spiral shape of the fiber. For simplicity we will still call the low-loss azimuthally polarized mode, the TE₀₁ mode, and the Gaussian-like fundamental mode, the HE₁₁ mode.

The TE₀₁ mode is the lowest-loss mode of cylindrical waveguides, and was first theoretically described by Carson *et al.* [2]. It is a linearly polarized azimuthal mode and has a doughnut shape with a harmonic null at its center. The TE₀₁ intensity distribution and its low loss make it an interesting mode for many applications, including atom guiding [13, 14] and high numerical aperture focusing [15, 16]. To generate a specific eigenfunction, or mode, like the TE₀₁, we utilize coupling misalignment and the filtering effect of band gap fibers. We define the coupling coefficient as the efficiency of coupling between the input beam and a fiber mode [17]:

$$\eta_c = \frac{1}{N} \int_A (\mathbf{E}_t^* \times \mathbf{H}_t' + \mathbf{H}_t^* \times \mathbf{E}_t') \cdot \hat{z} dA,$$

where η_c is the coupling coefficient, N is a normalization factor, E_t is the transverse component of the electric field, H_t is the transverse component of the magnetic field, and A is the infinite cross-section.

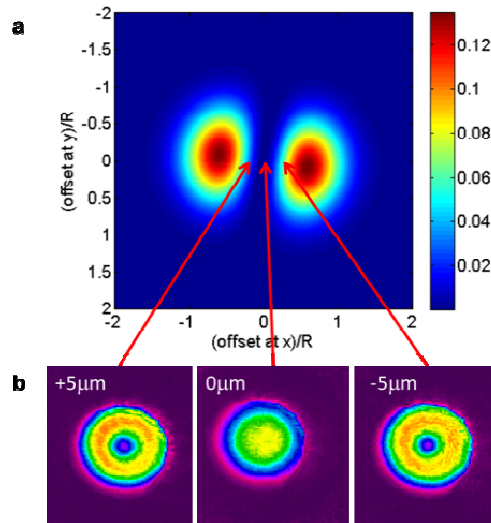


Fig. 1. (a). Coupling coefficient between linearly polarized Gaussian beam and the TE₀₁ mode as a function of offset. The offset is normalized by the fiber radius, R . (b) Measurement results of the mode at the output of the fiber at three offsets- center (0), 5 μm to the left of the center ($-0.2R$) and 5 μm to the right ($0.2R$).

We use the electric and magnetic fields, obtained by a finite element simulation of the spiral fiber (COMSOL), to calculate the coupling coefficient between a linearly polarized Gaussian beam and the spiral fiber TE₀₁ as a function of the coupling offset. The results for the spiral fiber are shown in Fig. 1(a). Note that these results are consistent with those obtained in other studies for the solid-core silica fiber [18, 19]. Similar calculations were done for a Bragg fiber showing comparable results. Since the input beam is linearly polarized and the TE₀₁ is an azimuthal mode, the coupling at the center of the fiber (offset zero) is negligible. The azimuthal polarization of the TE₀₁ also causes the coefficient to always be larger in one direction (in the example shown in the figure, right to left) than the other (up to down) because the integrand of the coupling coefficient will be larger when the polarization of the input beam and mode are parallel and will go to zero when they are perpendicular. As

seen in Fig. 1(a), the largest coupling coefficient is achieved at a coupling offset of $0.6R$ (where R is the fiber core radius), where 13.5% of the power couples to the TE_{01} . A coupling efficiency of 13.5% means that at the fiber input-facet the light is not coupled to a pure TE_{01} but is coupled to the TE_{01} along with a host of other modes. To achieve a pure TE_{01} at the output of the fiber we utilize the band gap filtering effect. This can be understood when examining the losses of the six lowest energy modes with respect to wavelength as shown in Fig. 2, calculated using the finite element simulation. Since the TE_{01} is the lowest-loss mode and the TE band gap is wider than the TM band gap, the ratio between the loss of the TE_{01} and the higher loss modes increases as it nears the edge of the band gap. Therefore, at the edge of the band gap the higher loss modes will be filtered out, leaving only the TE_{01} at the output of the fiber with a properly chosen length. The farther away from the center of the band gap, the stronger the filtering effect, and, therefore, a shorter fiber can be used. However, the farther from the center of the band gap, the higher the losses of the TE_{01} mode and the less power can be obtained at the output.

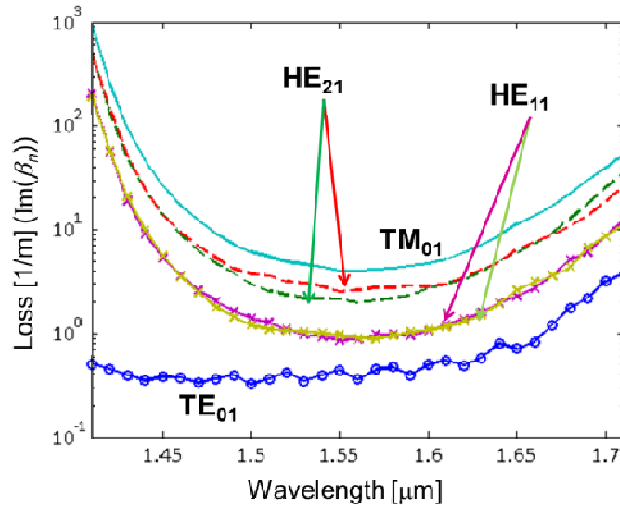


Fig. 2. Modes' losses as a function of wavelength – a result of the simulation. The ratio between the loss of the TE_{01} mode and the loss of the other modes becomes higher as we go further away from the center of the band gap (here at $1.56\mu\text{m}$).

Though we have shown here the effects of offsets, tilt is also examined, and it does not prevent the generation of TE_{01} but rather transforms the problem into an asymmetric problem (the intensity of the generated TE_{01} is different when the offset is at an angle θ or when it is at an angle $\theta + \pi$). Since our only concern is generating TE_{01} with the largest intensity, this can be easily overcome by optimizing the fiber position with respect to the beam in order to achieve the strongest output. Though the results are very similar to those of a Bragg fiber, there is a slight difference that results from the fact that the TE_{01} at the spiral fiber does not have the classical symmetric doughnut shape. The spiral TE_{01} has the same intensity distribution along the radius as the Bragg's TE_{01} (minimum intensity at the center), but the intensity along one axis is stronger than the intensity along the perpendicular axis (as shown in Fig. 3(d) and 3(e)). This means that aside from the dependence on the offset direction, the coupling coefficient also depends on the fiber orientation (or mode orientation). The variation from the doughnut shape is dependent on the position in the band gap; as the wavelength becomes shorter the mode becomes more doughnut shaped, reducing the added dependence on the fiber orientation.

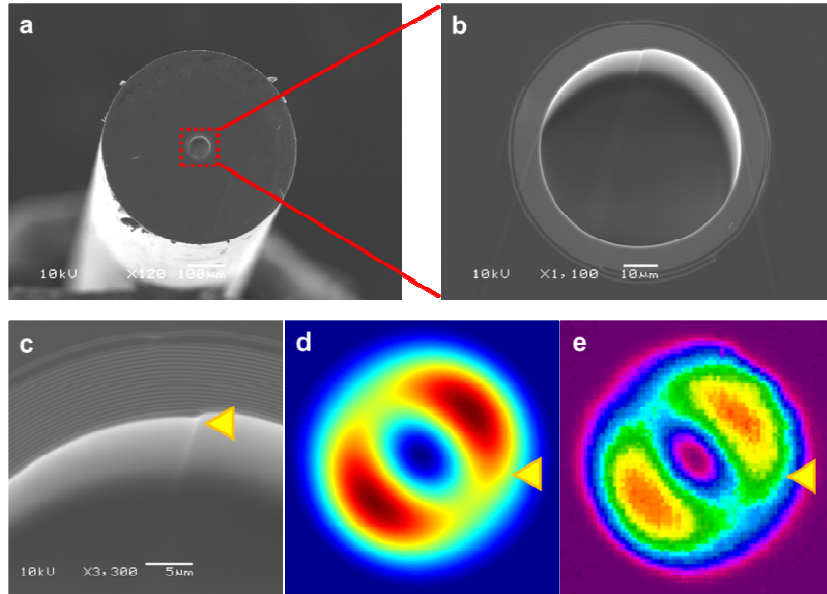


Fig. 3. (a) SEM of a spiral fiber (b) the hollow core and spiral bilayers- the light colored layers are made of chalcogenide glass (As_2S_3) the dark colored layers and cladding are made of poly(ether imide) (PEI). (c) The “seam” – the line that marks the beginning of the spiral (position marked by the yellow triangle) (d) Finite element simulation results – TE_{01} mode of spiral fiber. (e) Experimental results – TE_{01} as measured in a spiral fiber.

In our study we have used either polycarbonate (PC) or poly(ether imide) (PEI) as the low index-of-refraction material and chalcogenide glass, $As_{25}S_{75}$ or As_2S_3 , as the high index-of-refraction material. The chalcogenide glass is deposited on both sides of a sheet of polymer using evaporative deposition. The glass-polymer sheet is then rolled on a mandrel with subsequent polymer layers added for cladding. The entire structure is consolidated, and the rod is removed to create the preform. The preform is later processed in a draw tower to achieve many meters of fiber [9] that consist of hollow air core surrounded by alternating layers of glass and polymer. The cross section of the fiber, due to the rolling technique, is a spiral. Scanning electron microscope (SEM) pictures of a sample fiber cross section are shown in Fig. 3(a)–3(c).

To generate the TE_{01} we use a 17cm piece of spiral fiber with a 50 μ m diameter core. The fiber’s first band gap is at 1620nm, and it is made from PC and $As_{25}S_{75}$ [20]. A tunable laser beam (Ti:Sapph with OPO- Coherent Mira-900 and Mira-OPO) is collimated and spatially filtered into a clean Gaussian beam, which is coupled into the fiber through a 15cm focal length lens. After aligning the fiber with the beam to achieve a Gaussian-like output (an HE_{11} mode), the fiber is misaligned until TE_{01} appears with maximum intensity. The output is imaged onto a camera (Sensors unlimited SU320) using a 20x objective, and a linear polarizer is placed between the objective and the camera to verify the generation of an azimuthally polarized mode. A pure TE_{01} can be seen below 1520nm with a misalignment as small as 5 μ m. Figure 1(b) shows the measurement results of an HE_{11} , when the beam is centered, and a TE_{01} , when the beam is at an offset with respect to the fiber. Notably, the use of misalignment to achieve coupling to the TE_{01} means that the preparation of the setup is simpler since the system performance is not very sensitive to an accurate alignment, which eliminates a potentially laborious alignment procedure.

After using the coupler fiber to produce the TE_{01} beam and filter unwanted modes, we use its output beam as the input to the second fiber (“test” fiber). The good match between this beam and a TE_{01} mode of the fiber should allow coupling to a single mode and allow single-

mode transmission through this highly multi-mode fiber. A second fiber is not necessary- we can use a longer coupler fiber knowing that single mode is achieved after a certain length. This approach, though, has two disadvantages: (1) Single mode is only achieved after a short length of fiber rendering this first section useless for practical applications. (2) To achieve an efficient filtering it is preferred to couple at the edge of the band gap which will produce a relatively higher loss TE₀₁ with a shorter propagation length. Coupling to the TE₀₁ mode in the test fiber can be done at any point along the TE band gap, though the lowest losses will be achieved at the center of the band gap. Once the TE₀₁ is generated from the coupler, it can be treated as any other light source and can be coupled to the test fiber using the same means as are used to couple laser light. It is important to note that, as with coupling a laser beam directly to the fiber, the best coupling will be made when the size of the input beam matches the size of the mode it is coupled to. In the cases where the core sizes match, it is straightforward to butt-couple the two fibers in order to achieve good coupling. In our setup, we used a 50 μ m core, 75cm-long PEI / As₂S₃ spiral fiber with a center band gap of 1500nm as our test fiber. When coupled directly to the laser beam we see a pure HE₁₁ mode at the output, as expected when coupling at the center of the band gap.

The results of both the experiment and the simulation, done at 1480nm, are shown in Fig. 4 alongside the experimental setup. As with the coupler, a 20x objective is used to image the output of the test fiber onto the camera. A linear polarizer is rotated between the objective and camera to verify an azimuthally polarized mode.

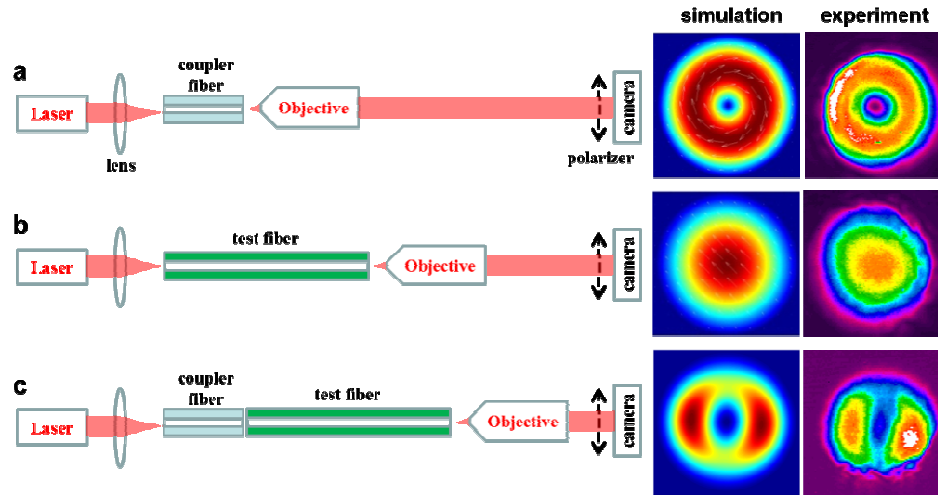


Fig. 4. Setup and results: on the left there is a schematic of the setup, in the center – simulation results and on the right the measurements results. (a) Laser coupled to the coupler fiber. The coupling is at an offset and the laser wavelength is at the edge of the fiber band gap, producing the TE₀₁ mode. (b) Laser is coupled to the test fiber. Setup is aligned and the laser wavelength is at the center of the test fiber band gap, producing the HE₁₁ mode. (c) Full setup- the coupler is butt-coupled to the test fiber.

It is important to note that the overall setup is very simple to construct and use. Since misalignment is needed to achieve the TE₀₁ in the coupler, very little attention is required in the setup. By working outside the band gap, to filter residual modes, we further reduce the need for careful alignment. Choosing the same core size for coupler and test fiber allows for butt-coupling and reduces the need for additional optical components and their positioning, and alignment. We have reduced the alignment to the tilt and position of one fiber with respect to the other, an alignment that is simplified by the transparency of the fibers' cladding and the use of an objective and camera aimed at the point where the two fibers meet.

Though the measurements here are done using a spiral photonic band gap fiber, the underlying methods and principals hold true for any type of band gap fiber. As mentioned above, once the coupler is used to achieve the azimuthally polarized beam, any circular waveguide that supports TE_{01} mode in the same wavelength range can be used, though adjustment to the beam size may be needed. This method allows us to achieve single-mode propagation even in cases of highly multi-mode waveguides as demonstrated here, allowing for many interesting applications. The setup and technique described here can easily allow guidance of particles using the TE_{01} mode to create a blue-detuned field [14]. Another interesting application can be dispersion compensation achieved by specially designed test fiber [21]. The described technique has many advantages, as it is not limited to any specific wavelength or core size, and, as shown in our experiments, it can allow guidance over relatively long fibers.

Acknowledgments

The authors would like to thank Professor Joannopoulos for his help and encouragement. This work was supported in part by the MRSEC Program of the US NSF under award number DMR-0819762 and also in part by the US Army Research Office through the ISN at MIT under contract no. W911NF-07-D-0004.